Journal of Magnetics 3(1), 4-8 (1998)

Thermal Behaviors of $Nd_2Fe_{14}B/Fe_3B$ Based Nanocomposite Magnets

ChoongJin Yang, EonByung Park and SeungDuck Choi

Electromagnetic Materials Lab., Research Institute of Industrial Science & Technology, P. O. Box 135, 790-600 Pohang, Korea

Gao Youhui and Zhu JingHan

Advanced Materials Institute, Central Iron & Steel Research Institute, Beijing 100081, P. R. China,

(Received 30 July 1997)

Two different compositions of melt spun magnetic alloys, $Nd_4Fe_{80}B_{16}$ and $Nd_4Fe_{76}Co_3Hf_{0.5}Ga_{0.5}B_{16}$, were characterized in terms of magnetic properties and thermal behaviors. It was found that the addition of Hf and Ga effectively slow down the crystallization rate of the nanocomposite $Nd_2Fe_{14}B/Fe_3B$ magnet. Coercivity($_iH_c$) changes only slightly with varying the post annealing conditions confirming that $_iH_c$ is not a sensitive magnetic quantity as a function of grain size and exchange coupled interaction. The experimentally observed behaviors of M_r and H_c do not vary monotonously with increasing grain size which is not in agreement with the numerically calculated result near the critical grain size(d_c). The plot of the grain size dependence for the remanence and coercivity in isotropic nanocomposite magnets has been revised in this study. The maxium energy product, $(B.H)_{max}=15.34$ MGOe, and a reduced remanence, $M_r/M_s=0.84$ were obtained, respectively.

1. Introduction

After the discovery of $Nd_2Fe_{14}B$ based rare earth magnetic compound melt spinning technique has led to an impact on commercializing the research results into industrialization[1~4]. Nowadays a wide variety of applications is possible due to the technological flexibility in producing the NdFeB bonded magnets with its quite affordable cost in producing the powders[5]. Although the recent rare earth permanent magnet can be obtained very high coercivity the remanence of these materials are limited to $M_s/2$ level due to the random grains distribution. This limitation was predicted long ago by Stoner and Wohlfarth[6].

Lately, the remanence in isotropic melt-spun NdFeB materials was reported to be enhanced by small addition of Si and Al[4, 7]. Recently many reports are exposed to have enhanced remanence larger than the Stoner-Wohlfarth limitation, $M_s/2=0.5$, in two-phased nanocomposite magnets [8~10]. The first one dimensional model to explain the superior magnetic behavior of the nanocomposite magnet was reported by Kneller and Hawig[11] who predicted that the highest coercivity can be achieved by exchange coupling force when the size of soft magnetic phase is twice as big as the domain wall width of the hard magnetic phase(~10 nm). In this case the reduced remanence(M_r/M_s) of the isopropic materials could be much larger than 0.5. To begin with the first report of Coehoorn et al. [10] a nanocomposite of $Nd_2Fe_{14}B/Fe_3B$ containing 70 % volume of the soft Fe_3B phase and the reduced remanence of 0.8 with a coercivity of 4 kOe was reported. More recently, Yang et al. [12] has indroduced a magnetic treatment to enhance the reduced remanence value up to 0.84 in the $Nd_2Fe_{14}B/Fe_3B$ nanocomposite materials containing Ga and Hf.

Magnetic characters of the nanocomposite magnets are influenced sensitively by their microstructures such as the volume ratio between hard and soft magnetic phases, the grain sizes and their uniform distribution[12~13]. Since the order of formation and growth rate of each phase, $Nd_2Fe_{14}B$, Fe_3B and α-Fe, is different, it is the key technology to get optium microstructure in the nanocomposite materials. In this study the effect of heat treating condition and the addition of Ga and Hf on the thermal behavior of the $Nd_2Fe_{14}B/Fe_3B$ based nanocomposite is reported.

2. Experiment

The ingots of $Nd_4Fe_{80}B_{16}$ and $Nd_4Fe_{76}Co_3Hf_{0.5}Ga_{0.5}B_{16}$ were prepared using metals in purity of Nd 99 %, FeB alloy (B 13 wt.%), Ga 99.9 %, Hf 99.5 %, and Co 99.5 %, respectively. These ingots were initially alloyed by arc melting for several times to obtain homogeneous composition, and then melt spun at a wheel speed of 26 m/sec. The thickness of ribbons was about 35 μm. The ribbons were identified to be completely amorphous by XRD analysis. The magnetic transformation and crystallization behaviors were detected by differential thermal analysis(DTA), and the magnetic thermal behavior was examined using a thermomagnetic analyzer(TMA) in the temperature range from 15 to 800 ℃. According to the DTA data, the melt spun ribbons were annealed at 650~750 ℃ for 2, 5, 10 and 15 minutes, respectively. The phase idendification was carried out by XRD, and the magnetic properties were characterized using a vibrating sample magnetometer applying an appropriate demagnetization factor. Microstructure was identified by taking high resolution transmission electron micrographs and the grain size was checked using an image analyzer.

3. Results and Discussion

A. Thermomagnetic Behaviors

By the differential thermal analysis scans both the samples of $Nd_4Fe_{80}B_{16}$ and $Nd_4Fe_{76}Co_3Hf_{0.5}Ga_{0.5}B_{16}$ were found to transform in two steps directly from amorphous to the final phases $Nd_2Fe_{14}B + Fe_3B + (\alpha\text{-Fe})$. However, the difference in crystallization temperature of the two samples is obvious in Fig. 1. Both the Hf and Ga are influential on the phase transformation temperature of nanocomposite alloy based of $Nd_2Fe_{14}B/Fe_3B$. For the curve of $Nd_4Fe_{80}B_{16}$ alloy two crystallization temperatures are observed at 582 and 618.2 ℃, and those of $Nd_4Fe_{76}Co_3Hf_{0.5}Ga_{0.5}B_{16}$ are 588.5 and 642.8 ℃. By the addition of Ga and Hf the both crystallization temperatures move up to a higher one and the interval between the first and second crystallization becomes wider from 36.2 to 54.3 ℃. To identify the first and second transformation, the $Nd_4Fe_{76}Co_3Hf_{0.5}Ga_{0.5}B_{16}$ samples were annealed for 5 minutes at 590 and 645 ℃, respectively, and then the phase was examined by XRD. The samples annealed at 590 ℃ still showed only the presence of α-Fe. However, those annealed at 645 ℃ exhibited the presences of $Nd_2Fe_{14}B$ and Fe_3B in addition to α-Fe. Therefore the first and second exothermal peak in Fig. 1 are the transformations from amorphous material to α-Fe and $Nd_2Fe_{14}B/Fe_3B$, respectively. However, it was difficult to distinguish the chronicle order of formation between $Nd_2Fe_{14}B$ and Fe_3B. Although the composition is not the same, Kneller et al. [11] confirmed that the amorphous $Nd_{3.8}Fe_{73.3}V_{3.9}Si_{1.0}B_{18}$ and $Nd_{3.8}Fe_{77.2}B_{19}$ ribbons exhibited the transformations in the order of $Fe_{23}B_6$, Fe_3B $Nd_2Fe_{14}B$ and finally α-Fe. In this study and the previous reports[12, 13] no formation of $Fe_{23}B_6$ was observed, rather the formation of Fe_3B was prominent after annealing.

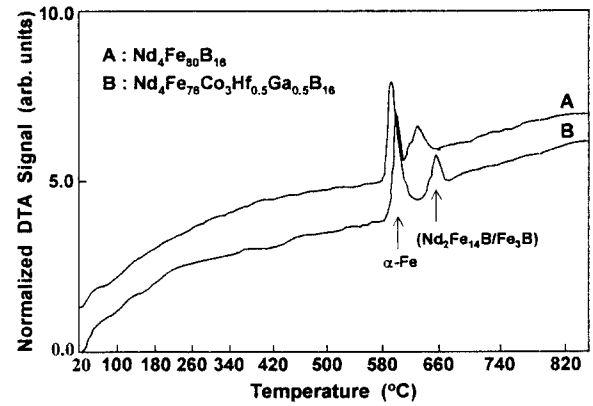

Fig. 1. DTA scan patterns of as-spun (A) $Nd_4Fe_{80}B_{16}$ and (B) $Nd_4Fe_{76}Co_3Hf_{0.5}Ga_{0.5}B_{16}$ ribbons performed at a scan rate of 10 ℃/min.

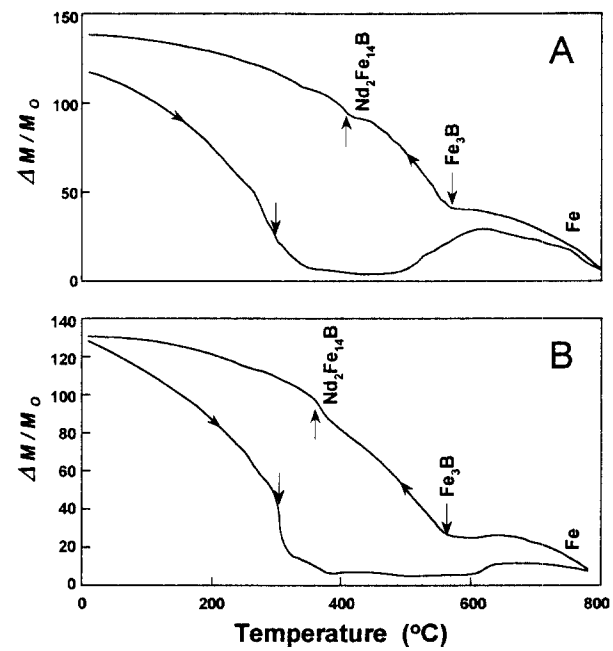

Fig. 2. The thermomagetization behaviors for the as-spun ribbons of (A) $Nd_2Fe_{14}B_{16}$, and (B) $Nd_4Fe_{76}Co_3Hf_{0.5}Ga_{0.5}B_{16}$, respectively.

The similar behaviors were characterized by thermomagnetic analysis (TMA) in Fig. 2. during heating the amorphous alloy and cooling the same sample. $\triangle M/M$ means the arbitrary unit which is normalized with respect to the initial magnetic force applying to the balance. During heating the both alloys in Fig. 2(A) and (B), the first change of magnetization can be seen to take place near 340 ℃ corresponding to the Curie tempertaure of $Nd_2Fe_{14}B$ phase formed from amorphous matrix. Upon heating further to about 600 ℃ a rise in magnetization takes place which is due to the formation of Fe_3B and probably the further formation of α-Fe. This explanation can be rationalized by cooling the same alloys reversely.

During cooling magnetization rises near 580~600 ℃ were obviously demonstrated which are corresponding to the Curie temperature of tetragonal Fe_3B phase[8].

B. Magnetic Behaviors

The typical demagnetization curves are shown in Fig. 3(a), (b) and (c). Each sample was annealed for 2(A), 5(B), 10(C) and 15(D) minutes at 650, 680, 700 and 750 ℃, respectively. A constriction along the magnetization curve at H = 0 was observed for the sample annealed at 700 ℃/(10, 15) min, 720 ℃/(5, 10, 15) min and 750 ℃/(2, 5, 10, 15) min as reported by Yang et al. [12, 13]. The other samples annealed at a lower temperature do not show the same behaviors as shown in Fig. 3. It has been analysed that the grain size is fine enough to have a strong exchange coupling due to the low temperature annealing just around the transformation temperature of the hard magnetic phase. Only the samples annealed at 650 ℃ for 2 minutes showed a constriction at H = 0 which seems to be due to the presence of remanent amorphous phase. It is also found that the annealing treatment below the second transformation temperature shown in Fig. 1, which are 680 and 650 ℃ for the sample $Nd_4Fe_{75.2}Co_3Hf_{0.5}Ga_{0.5}B_{16.8}$ and $Nd_4Fe_{80}B_{16}$, respectivley, has a great effect on enhancing the remanence, rather less effect on the coercivity. The annealing above the second transformation temperature turned out to have no influence.

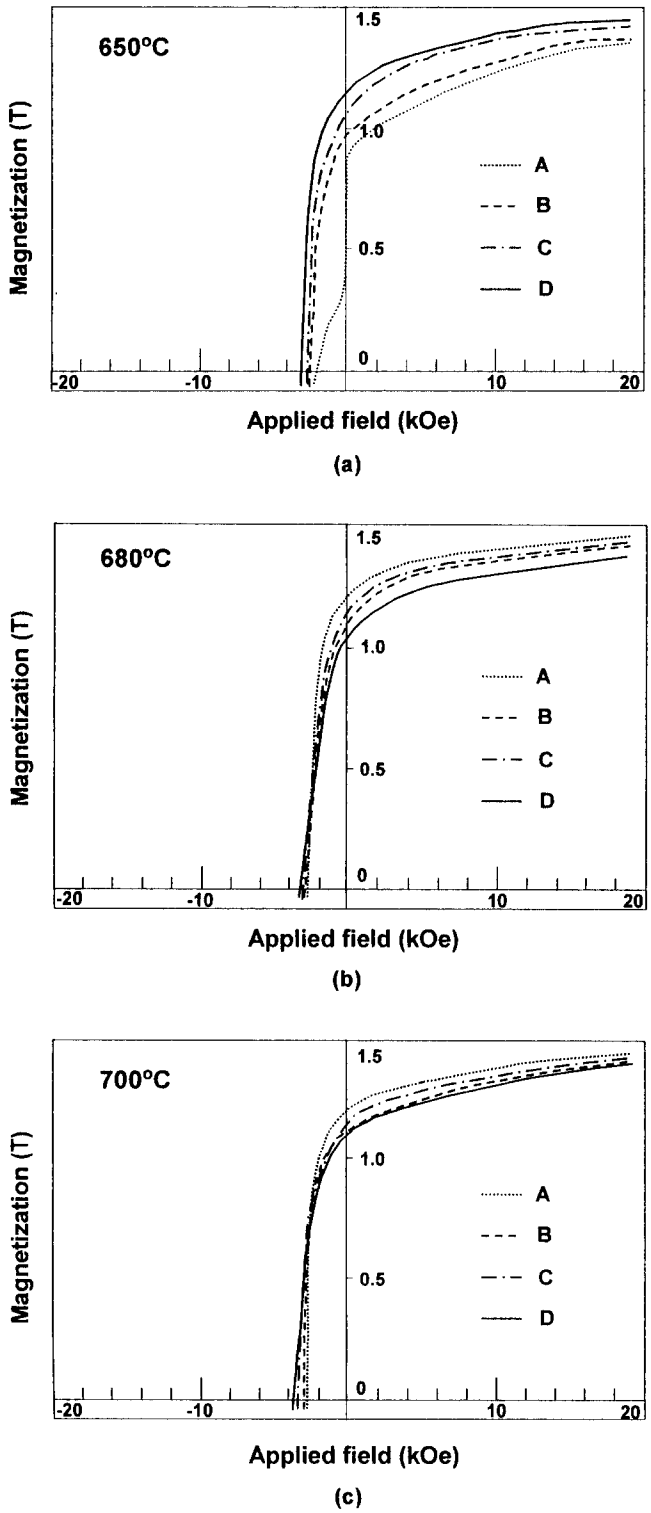

Fig. 3. Demagnetization curves of the as-spun $Nd_4Fe_{76}Co_3Hf_{0.5}Ga_{0.5}B_{16}$ ribbons annealed at (a) 650 ℃, (b) 680 ℃ and (c) 700 ℃ for 2(A), 5(B), 10(C) and 15(D) minutes, respectively.

Fig. 4(A) and (B) summarize the magnetic properties of the alloys $Nd_4Fe_{76}Co_3Hf_{0.5}Ga_{0.5}B_{16}$ and $Nd_4Fe_{80}B_{16}$, respectively, as a function of annealing temperature and time. In general, both the saturation and remanent magnetization for $Nd_4Fe_{80}B_{16}$ alloys show higher values than those of $Nd_4Fe_{76}Co_3Hf_{0.5}Ga_{0.5}B_{16}$ alloys annealed under an identical condition. The insets a, b, c and a′, b′, c′, respectively, denote the detailed remanence values varying as a function of annealing time at a given temperature for the alloys $Nd_4Fe_{76}Co_3Hf_{0.5}Ga_{0.5}B_{16}$ and $Nd_4Fe_{80}B_{16}$. Although the variations in M_s and M_r do not show a commom trends for both the alloys, the highest values in both M_s and M_r are obtained from the samples annealed for 2 min or 5 min at a lower tempertaure (680~700 ℃) annealing. Particularly the maximum M_s values for the alloys are obtained at 680 ℃ and 700 ℃ annealing, respectively. The highest M_r value which is obtained from (680 ℃ /2 min) annealing for $Nd_4Fe_{76}Co_3Hf_{0.5}Ga_{0.5}B_{16}$ is 12.0 kG, while the highest M_r of $Nd_4Fe_{80}B_{16}$ obtained from (700 ℃/2 min) annealing is 12.5 kG. Taking into account the variations of M_r shown in the insets a, b, c, a′, b′ and c′ in Fig. 4(A) and (B), the simulated variation of remanence values proposed by Schrefl et al. [14] can be revised such that the remanence does not decrease monotonously rather it decreases rapidly to a certain lower value and then shows a plateau without a prominent change until an optimized grain size is obtained. The insets b′ and c′ in Fig. 4. also show that M_r then tends to decrease again monotonously which is seen in Fig. 5, too. It must be noticed that a prolonged annealing over 10 minutes is not desirable for the both alloys.

Fig. 5 shows the grain size effect on the magnetic properties of nanocrystalline $Nd_2Fe_{14}B/\ \alpha$-Fe magnets by Schrefl et al. [14] comparing numerically calculated data and $Nd_2Fe_{14}B/Fe_3B$ magnet used in this study. The remanence(open circle) decreases while the coercivity(solid circle) increases monotonously with increasing the grain size as can be seen in Fig. 5. The variations in both remanence and coercivity below a critical grain size, $d_c = 22$ nm, are

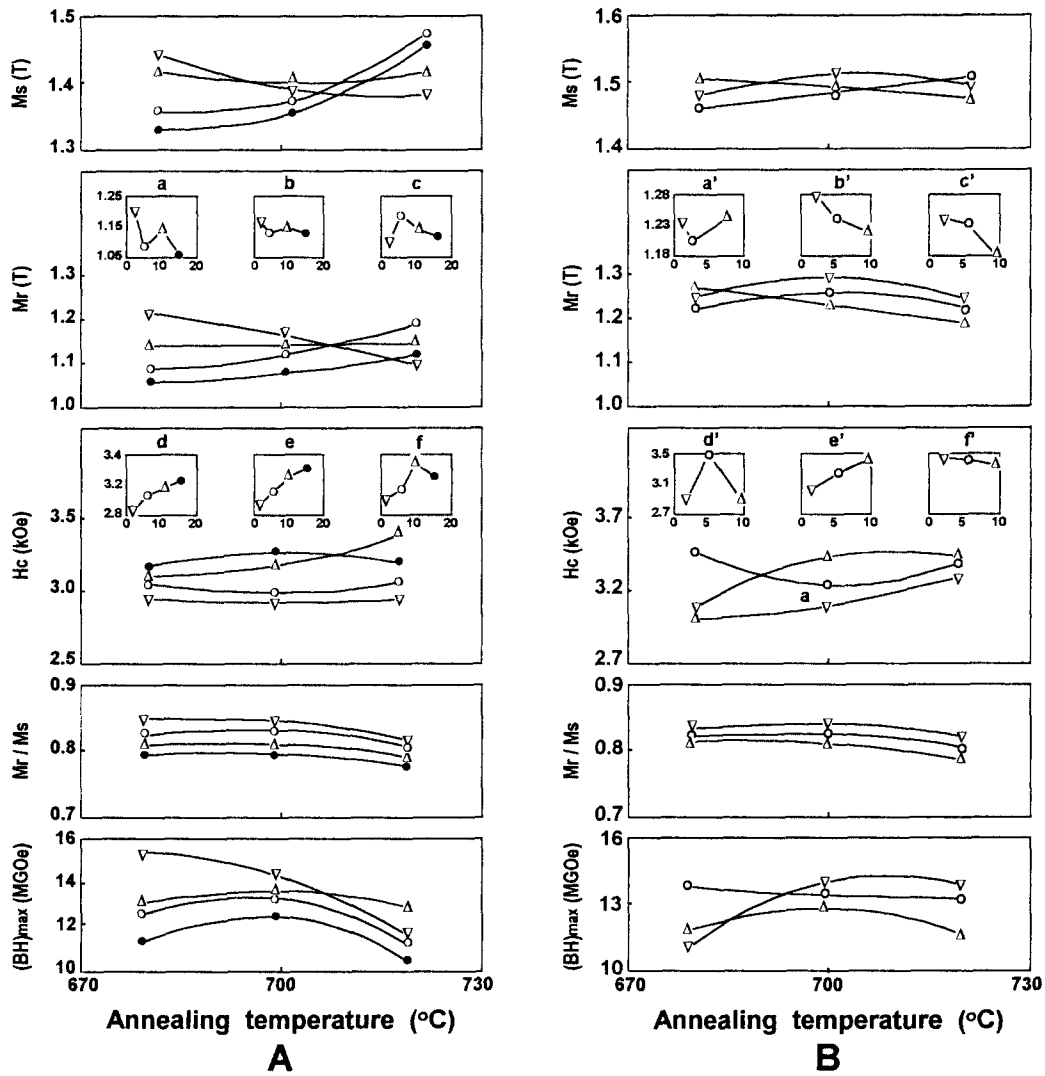

Fig. 4. The variation of magnetic properties for the two series of samples (A) $Nd_4Fe_{76}Co_3Hf_{0.5}Ga_{0.5}B_{16}$ and (B) $Nd_4Fe_{80}B_{16}$ annealed at different temperatures and times. The symbols in the insets denote the annealing time; ▽ 2 min, ○ 5 min, △ 10 min, and ● 15 min, respectively.

more prominent. It can be inferred from the hysteresis curves that the grain size annealed below the second transformation temperature in Fig. 1 is finer than d_c, while that of samples annealed above the second transformation temperature is coarser than d_c. Since the second transformation temperature of the alloy $Nd_4Fe_{76}Co_3Hf_{0.5}Ga_{0.5}B_{16}$ is higher than that of $Nd_4Fe_{80}B_{16}$, it is also regarded that Hf and Ga can slow down the grain growth. Above d_c, however, the coercivities are not markedly dependent upon the annealing condition, while the remanence is still sensitive to it. Due to the role of Hf and Ga on slowing down the grain growth, annealing the alloy $Nd_4Fe_{76}Co_3Ga_{0.5}Hf_{0.5}B_{16}$ at 650 ℃ for 2 minutes resulted in incomplete crystallization having residual amorphous material while the alloy $Nd_4Fe_{80}B_{16}$ showed a complete crystallization. The $Nd_4Fe_{76}Co_3Hf_{0.5}Ga_{0.5}B_{16}$ alloy showed a constriction along the demagnetization curve at $H=0$, and accordingly a lower M_s as well as shown in Fig. 3(a).

Unlike the M_s and M_r behaviors, the addition of Hf and Ga allows the alloy to have a highest coercivity 3.4 kOe by a prolonged annealing at 720 ℃ for 10 minutes. However, due to the lower M_r at the same annealing condition the highest $(B.H)_{max}=15.2$ MGOe are obtained from the sample annealed at 680 ℃ for 2 minutes for the $Nd_4Fe_{76}Co_3Hf_{0.5}Ga_{0.5}B_{16}$ alloy, while the highest $(B.H)_{max}=14.5$ MGOe are obtained from (700 ℃/2 min) annealing for the $Nd_4Fe_{80}B_{16}$ alloy where the maximum coercivity is exhibited. Consequently the variation of coercivity values is not monotonous as was simulated by Schrefl et al. [14]. For many compositions of nanocomposite alloys coercivity starts to increase with increasing the grain size, which is of course as a function of annealing time, and then exhibits a peak value at an optimized grain size. Thereafter, the coercivity values tend to decrease slightly with prolonged time of annealing.

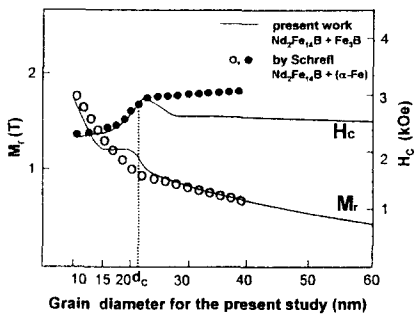

Fig. 5. The revised comparison of magnetization and coercivity variations as a function of grain size for the nanocomposite magnets of the present study and Schrefl's simulation.

This behavior is clearly seen in the insets d, e, f, d′, e′ and f′ shown in Fig. 4(A) and (B). It is interesting, however, that the coercivity starts to show a peak value where remanence value starts to decrease slowly from a plateau stagnated change. In short, there is some discrepancy between the experimental results and the simulated behavior in the variations of remanence and coercivty as well. Therefore the revised variation curves are proposed in this study as shown in Fig. 5. In Fig. 5 the solid lines denote the variations of H_c and M_r of the present alloy which is nanocomposite of $Nd_2Fe_{14}B/Fe_3B$, while the dotted lines of circles are for the nanocomposite of $Nd_2Fe_{14}B/(\alpha\text{-Fe})$. Fig. 6 is a high resolution TEM micrograph showing the nanocrystalline $Nd_2Fe_{14}B$ grains embedded by soft magnetic Fe_3B and α-Fe grains.

Fig. 6. High resolution TEM micrograph showing the nanocomposite structure of $Nd_4Fe_{76}Co_3Hf_{0.5}Ga_{0.5}B_{16}$ magnets of about the critical grain size, 22 nm.

As was noted in references [12, 13], a reduced remanences value more than 0.84 again is obtainable in these $Nd_4Fe_{76}Hf_{0.5}Ga_{0.5}B_{16}$ alloys by an appropriate annealing treatment.

4. Conclusion

The additions of Hf and Ga were found to slow down the crystallization rate in nanocomposite $Nd_2Fe_{14}B/Fe_3B$ base alloys. The variation of M_s and M_r values are sensitively change with increasing the grain size, i.e, as a function of annealing time or temperature, while coercivity values show rather a less sensitive change as a function of grain size. However, both the M_r and H_c exhibit a plateau and a peak value, respectively, along the variation curves eventhough the temperature where the peak takes place are not identical. The highest $M_r/M_s = 0.84$ were obtained for the $Nd_4Fe_{76}Co_3Hf_{0.5}Ga_{0.5}B_{16}$ annealed at 680 ℃ for 2 minutes and for the $Nd_4Fe_{80}B_{16}$ annealed at 700 for 2 minutes, respectively. These conditions allow those alloys to exhibit the $(B.H)_{max}$ = 15.3 MGOe and 14.6 MGOe, respectively.

References

[1] J. J. Croat, J. F. Herbst, R. W Lee, and F. E. Pinkerton, J. Appl. Phys. **55**, 2078 (1984).

[2] R. W. Lee, Appl. Phys. Lett., **46**, 790 (1985).

[3] R. W. Lee, E. G. Brewer, and N. A. Schaffel, IEEE Trans. Magn., **MAG21**, 1958 (1985).

[4] R. W. McCallum, A. M. Kadin, and J. E. Keem, J. Appl. Phys., **61**, 3577 (1987).

[5] W. Hart and P. Wheeler, Proc. of 9th Inter. Business Conference on NdFeB '95, Gorham/Intertech Consulting, San Diego, Calf., Feb. 26~28 1995, eds. Gorham Institute.

[6] E. C. Stoner and E. P. Wohlfarth, Philos. Trans. R. Soc. London, Ser. **A 240**, 599 (1948).

[7] G. C. Hadjipanys and W. Gong, J. Appl. Phys., **64**, 5559 (1988).

[8] R. Coehoorn, D. B. DeMooji, and D. DeWaard, J. Magn. Magn. Mater., **80**, 101 (1989).

[9] J. Ding, P. G. McCormick, and R. Street, J. Magn. Magn. Mater., **124**, 1 (1993).

[10] L. Withanawasam, G. C. Hadjipanys, and R. F. Krause, J. Appl. Phys., **75**, 6646 (1994).

[11] E. F. Kneller and R. Hawig, IEEE Trans. Magn., **MAG-27**, 3588 (1991).

[12] C. J. Yang and E. B. Park, IEEE Trans. Magn., **MAG-32** (5) 4428 (1996).

[13] C. J. Yang and E. B. Park, J. Magn. Magn. Mater., **166**(2) 243 (1997).

[14] T. Schrefl, J. Fidler, and H. Kronmuller, Phys. Rev. B, **49** (9) 6100 (1994).